ACOUSTICS 2012

Acoustic modulation effect of rotating stator/rotor interaction noise

A. Gerard, S. Moreau, A. Berry and P. Masson

GAUS, Université de Sherbrooke, 2500 Boul. de l'Université, Sherbrooke, Canada J1K2R1
anthony.gerard@usherbrooke.ca

Tonal noise from fans mainly comes from the periodic unsteady blade forces and/or vane forces due to the interaction between the rotor and its environment. To distinguish the different interactions leading to tonal noise in the acoustic spectrum, this paper presents an original method consisting of rotating a quasistatic part, e.g. a stator or an obstruction in the environment of the rotor. An analytical model has been developed to take into account relative rotation motions between a number of rotors. This model shows that the acoustic radiation due to the interaction between a rotating stator and the rotor shifts in the spectrum at frequencies $\omega = mB^{(k)}\Omega^{(k)} - n\Omega^{(l)}$, where m is the harmonic order, $B^{(k)}$ is the number of rotor blades, $\Omega^{(k)}$ is the angular velocity of the rotor, $\Omega^{(l)}$ is the angular velocity of the moving quasistatic part and n is the order of the unsteady forces decomposed in circumferential Fourier series. Using this modulation effect, every circumferential mode n radiates at different frequency in the acoustic spectrum. The radiation due to the interaction between the rotor and all the other static components remains at frequencies $mB^{(k)}\Omega^{(k)}$.

1 Introduction

Fans are composed of a rotating part and statoric parts. The fluid interaction between the various components of the fan lead to fluctuating forces on the rotor blades and on the fixed parts. According to the Ffowcs-Williams and Hawkings analogy, the surface forces can be seen as a distribution of elementary dipoles. For subsonic fans, tonal noise mainly comes from the periodic forces on the rotor blades and the forces on the other static parts of the fan (e.g. stator). As derived in analytical models and measured experimentally, the tonal noise emitted by every component of the fan system radiates at the Blade Passage Frequency (BPF) and its harmonics [1-8]. This coincidence make difficult the discrimination of tonal noise sources.

This paper aims at giving new analytical and experimental tools to discriminate the sources of tonal noise emitted from the fan system. The approach proposed in this paper consists of rotating one of the fixed part of the fan to create tonal noise modulation. The analysis of the frequency shifts caused by this modulation can lead to source discrimination (stator, rotor, environment) and gives information about the circumferential modal content of the forces responsible for tonal noise.

The analytical formulation is first developed and illustrated by simulation results. Then experiments involving a rotating rectangular obstruction interacting with an axial fan is presented.

2 Analytical model for tonal noise modulation

2.1 Formulation

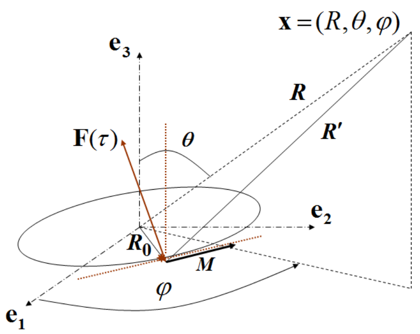

Figure 1: Coordinate system.

In this section, the acoustic pressure field radiated by K coaxial rotors in free field is derived. We consider that only aerodynamic forces on the fan blades radiate sound for low speed fans [1][2][3][4], therefore quadripolar and monopolar sources are neglected. The blade force sources are considered concentrated on a mean radius R_0. This is typically valid as long as the acoustic wavelength of the emitted sound is much larger than the radial extent of the blade span. The main source in the Ffowcs Williams and Hawkings analogy for subsonic fans is therefore the dipolar term associated with the distribution of forces applied by the blades on the fluid [3]. Periodic forces lead to discrete tone generation while random forces lead to broadband noise. In either case, the acoustic pressure radiated by a compact rotating dipole can be expressed as follows in the frequency domain (Cf. Fig. 1):

$$\tilde{p}(\mathbf{x}, \omega) = \frac{i\omega}{8\pi^2 c_0} \int_{-\infty}^{+\infty} \frac{\mathbf{F}\mathbf{R}'}{R'^2} e^{i\omega(\tau + R'(\tau)/c_0)} d\tau \tag{1}$$

where $\mathbf{x} = (R, \theta, \varphi)$ is the reception point in spherical coordinate, τ is the emission time, ω is the angular frequency, c_0 is the speed of sound. The point force vector $\mathbf{F}$ is defined by its component along the cartesian referential $(\mathbf{e_1}, \mathbf{e_2}, \mathbf{e_3})$ of the source, where $\mathbf{e_3}$ is the axial direction of the fan and $(\mathbf{e_1}, \mathbf{e_2})$ belongs to the plane of rotation:

$$\begin{aligned}\mathbf{F} = [&F_r \cos(\Omega\tau + \varphi_0) - F_t\theta \sin(\Omega\tau + \varphi_0), \\ &F_r \sin(\Omega\tau + \varphi_0) + F_t\theta \cos(\Omega\tau + \varphi_0), F_a]\end{aligned} \tag{2}$$

where the indices r, t and a denotes the radial, tangential and axial direction of the forces in the cylindrical referential respectively and φ_0 is the circumferential angle of the dipole point at $\tau = 0$. In Eq. (1), the distance vector $\mathbf{R}'$ between the emitter and the receiver is defined by:

$$\begin{aligned}\mathbf{R}' = \mathbf{R} - \mathbf{R_0} = [&R \sin\theta \cos\varphi - R_0 \cos(\Omega\tau + \varphi_0), \\ &R \sin\theta \sin\varphi - R_0 \sin(\Omega\tau + \varphi_0), R\cos\theta]\end{aligned} \tag{3}$$

where R is the scalar distance between the origin and the receiver and R_0 is the scalar distance between the origin and the emitter, as shown in Fig. 1. Using the far field approximation $R' = R - R_0 \sin\theta \cos(\Omega\tau - \varphi + \varphi_0)$, replacing $\mathbf{F}$ and $\mathbf{R}'$ in Eq. (1) and using the Jacobi-Anger expansion $e^{ia\cos\psi} = \sum_{\nu=-\infty}^{+\infty} (i)^\nu J_\nu(a) e^{i\nu\psi}$ lead to the following expression of the acoustic pressure:

$$\begin{aligned}\tilde{p}(\mathbf{x},\omega) &= \frac{i\omega e^{i\omega R/c_0}}{4\pi c_0 R}\sum_{\nu=-\infty}^{+\infty}(-i)^{\nu}e^{i\nu(\varphi-\varphi_0)} \\ &\times \left[i\sin\theta J'_{\nu}\left(\frac{\omega R_0\sin\theta}{c_0}\right)\tilde{F}_r(\omega-\nu\Omega)\right. \\ &+ \left.\left(\cos\theta\tilde{F}_a(\omega-\nu\Omega)-\frac{\nu c_0\tilde{F}_t(\omega-\nu\Omega)}{\omega R_0}\right)J_{\nu}\left(\frac{\omega R_0\sin\theta}{c_0}\right)\right]\end{aligned} \tag{4}$$

where J_ν is the ordinary Bessel function of order ν and its derivative $J'_\nu(a) = \frac{1}{2}(J_{\nu-1}(a) - J_{\nu+1}(a))$.

The Fourier transform of a periodic force acting on the b^{th} blade of a $B-$bladed rotor can be expressed as:

$$\tilde{F}(\omega) = \sum_{n=-\infty}^{+\infty} F_n e^{-in\frac{2\pi b}{B}}\delta(\omega - n\Omega) \tag{5}$$

where the initial phase φ_0 is replaced by $2\pi b/B + \varphi_0^{(b)}$ for the b^{th} blade (with $\varphi_0^{(b)} = 0$ for a sake of simplicity) and F_n are the Fourier circumferential coefficients given by :

$$F_n = \frac{\Omega}{2\pi}\int_0^{2\pi/\Omega} F(t)e^{in\Omega t}dt \tag{6}$$

where n is the circumferential order of the blade force.

If the k^{th} row, rotating at angular velocity $\Omega^{(k)}$ experiences forces due to the l^{th} row rotating at $\Omega^{(l)}$, then $\Omega = \Omega^{(k)} - \Omega^{(l)}$. Inserting Eq. (5) into Eq. (4) and considering $B^{(k)}$ blades equally spaced in the k^{th} rotor row, the acoustic radiation of the k^{th} row due to the interaction with the l^{th} row can be expressed by:

$$\begin{aligned}[\tilde{p}(\mathbf{x},\omega)]^{(k)\leftarrow(l)} &= \sum_{n=-\infty}^{+\infty}\sum_{\nu=-\infty}^{+\infty}\sum_{b=1}^{B^{(k)}}\frac{i\omega e^{i\omega R/c_0}}{4\pi c_0 R}(-i)^{\nu}e^{i\nu\varphi}e^{-i(n+\nu)\frac{2\pi}{B^{(k)}}b} \\ &\times \left[i\sin\theta F_{r,n}^{(k)\leftarrow(l)}J'_{\nu}\left(\frac{\omega R_0\sin\theta}{c_0}\right)\right. \\ &+ \left.\left(\cos\theta F_{a,n}^{(k)\leftarrow(l)}-\frac{\nu c_0}{\omega R_0}F_{t,n}^{(k)\leftarrow(l)}\right)J_{\nu}\left(\frac{\omega R_0\sin\theta}{c_0}\right)\right]\end{aligned} \tag{7}$$

where $F_{a,n}^{(k)\leftarrow(l)}$, $F_{t,n}^{(k)\leftarrow(l)}$, $F_{r,n}^{(k)\leftarrow(l)}$ are the n^{th} mode of the axial, tangential and radial components of the forces respectively and $\omega = n\left(\Omega^{(k)} - \Omega^{(l)}\right) + \nu\Omega^{(k)}$.

Considering that the unsteady loading is the same on each blade and since $\sum_{b=1}^{B^{(k)}} e^{-i(n+\nu)(2\pi/B^{(k)})b} = \sum_{m=-\infty}^{+\infty} B^{(k)}\delta(n+\nu - mB^{(j)})$ is null if $\nu \neq mB^{(k)} - n$, the acoustic pressure field due to forces acting on the k^{th} rotor blades coming from a l^{th} rotor periodic flow is :

$$\begin{aligned}[\tilde{p}(\mathbf{x},\omega)]^{(k)\leftarrow(l)} &= \sum_{m=-\infty}^{+\infty}\sum_{n=-\infty}^{+\infty}\frac{i\omega e^{i\omega R/c_0}B^{(k)}}{4\pi c_0 R}(-i)^{(mB^{(k)}-n)}e^{i(mB^{(k)}-n)\varphi} \\ &\times \left[i\sin\theta F_{r,n}^{(k)\leftarrow(l)}J'_{mB^{(k)}-n}\left(\frac{\omega R_0\sin\theta}{c_0}\right)\right. \\ &+\left(\cos\theta F_{a,n}^{(k)\leftarrow(l)}-\frac{(mB^{(k)}-n)c_0}{\omega R_0}F_{t,n}^{(k)\leftarrow(l)}\right) \\ &\left.\times J_{mB^{(k)}-n}\left(\frac{\omega R_0\sin\theta}{c_0}\right)\right]\end{aligned} \tag{8}$$

with $\omega = mB^{(k)}\Omega^{(k)} - n\Omega^{(l)}$.

Finally, if the acoustic pressure field radiated by K radiating rotors due to flow disturbances originating from L rotors can be linearly superimposed, the total pressure field can be written:

$$\tilde{p}(\mathbf{x},\omega) = \sum_{k=1}^{K}\sum_{l=1}^{L}\left[\tilde{p}(\mathbf{x},\omega)\right]^{(k)\leftarrow(l)} \tag{9}$$

2.2 Comparison to other models

This formulation is consistent with the tonal noise model presented in [5] for Counter Rotating Open Rotors (CROR), if the forward flight speed is neglected. In this case, $B^{(k)}$ and $B^{(l)}$ are the rear-rotor and front-rotor numbers of blades respectively and $\Omega^{(k)}$ and $\Omega^{(l)}$ are the rear-rotor and front-rotor angular velocities respectively. Eq. (8) can be used to calculate the sound radiated by the rear-rotor caused by the periodic wakes shed by the front rotor by replacing n by $nB^{(l)}$, since the circumferential harmonic content of the front rotor wake are integer multiples of the front-rotor number of blades $B^{(l)}$, thus $\omega = mB^{(k)}\Omega^{(k)} + nB^{(l)}\Omega^{(l)}$ (where the sign + comes from the counter rotation of the rotors).

If the radial forces are neglected, Eq. (8) is also consistent with Lowson's model for compressor stages [1], for both noise radiation from the rotor and the stator. In the case of stator/rotor interaction noise: $\Omega^{(l)} = 0$, thus $\omega = mB^{(k)}\Omega^{(k)}$, which means that all the circumferential orders of the force radiate at the same frequencies. Moreover, since the circumferential harmonic content of the stator wake are integer multiples of the number of the stator vanes $B^{(l)}$, n can be replaced by $nB^{(l)}$.

In the particular case of rotor/stator interaction ($\Omega^{(k)} = 0$), the circumferential order n of the forces exerted on the non-rotating k^{th} row due to the rotating $B^{(l)}-$bladed l^{th} row becomes $nB^{(l)}$, thus $\omega = -nB^{(l)}\Omega^{(l)}$ and the acoustic pressure radiated by row (k) due to the interaction with row (l), provided by Eq. (8), is equivalent to the analytic formulation of stator noise given by Lowson [1].

The proposed formulation is also equivalent to the loading noise model developed in [6] for centrifugal fans (if only one row rotates).

Thus, the noise radiation from a rotor, a stator or a CROR and from axial or centrifugal fans are particular cases of the multi-row rotors derived in this section.

2.3 Discretization

In order to perform simulations, Eq. (8) is discretized as follows:

$$\begin{pmatrix} p_{\omega 1}^{(k)\leftarrow(l)} \\ \vdots \\ p_{\omega j}^{(k)\leftarrow(l)} \\ \vdots \\ p_{\omega J}^{(k)\leftarrow(l)} \end{pmatrix} = \begin{pmatrix} \bar{\mathbf{H}}_{\omega\mathbf{11}} & \dots & \bar{\mathbf{H}}_{\omega 1i} & \dots & \bar{\mathbf{H}}_{\omega 1I} \\ \vdots & & \vdots & & \vdots \\ \bar{\mathbf{H}}_{\omega j1} & \dots & \bar{\mathbf{H}}_{\omega ji} & \dots & \bar{\mathbf{H}}_{\omega jI} \\ \vdots & & \vdots & & \vdots \\ \bar{\mathbf{H}}_{\omega J1} & \dots & \bar{\mathbf{H}}_{\omega Ji} & \dots & \bar{\mathbf{H}}_{\omega JI} \end{pmatrix} \begin{pmatrix} \bar{\mathbf{F}}_{n1}^{(k)\leftarrow(l)} \\ \vdots \\ \bar{\mathbf{F}}_{ni}^{(k)\leftarrow(l)} \\ \vdots \\ \bar{\mathbf{F}}_{nI}^{(k)\leftarrow(l)} \end{pmatrix} \tag{10}$$

with :

$$\bar{\mathbf{H}}_{\omega ji} = [H_{r,\omega ji}, H_{t,\omega ji}, H_{a,\omega ji}]$$

where the subscripts a is for axial, t for tangential, r for radial, ω for the acoustic frequency, j for the discretized acoustic field point, n for the circumferential order of the force (also called mode order in the following) and i for the index of the radial discretization of the row (k)

$$H_{r,\omega ji} = H_{\omega j} \sin\theta_j J'_{mB^{(k)}-n}\left(\frac{\omega R_{0i}\sin\theta_j}{c_0}\right) \quad (11)$$

$$H_{t,\omega ji} = H_{\omega j}\frac{(mB^{(k)}-n)c_0}{\omega R_{0i}} J_{mB^{(k)}-n}\left(\frac{\omega R_{0i}\sin\theta_j}{c_0}\right) \quad (12)$$

$$H_{a,\omega ji} = H_{\omega j} \cos\theta_j J_{mB^{(k)}-n}\left(\frac{\omega R_{0i}\sin\theta_j}{c_0}\right) \quad (13)$$

with :

$$H_{\omega j} = \frac{i\omega e^{i\omega R_j/c_0} B^{(k)}}{4\pi c_0 R_j}(-i)^{(mB^{(k)}-n)} e^{-i(mB^{(k)}-n)\varphi_j}$$

and:

$$\bar{\mathbf{F}}_{ni} = \begin{pmatrix} F_{r,ni} \\ F_{t,ni} \\ F_{a,ni} \end{pmatrix}$$

From Eq. (10), there is a little gap to use this model to estimate the unsteady forces from measured acoustic pressure following the procedure described in [7].

2.4 Simulation

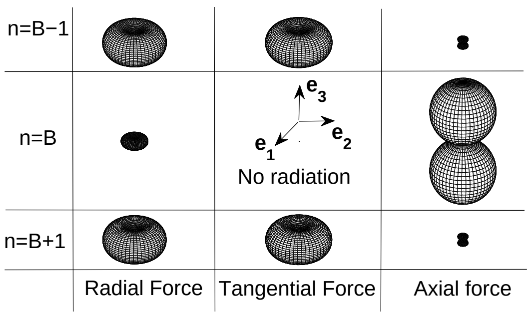

Figure 2: Simulated directivities from Eq. (10). Left to right: $\bar{\mathbf{F}}_{\mathbf{n1}} = [1\text{N}, 0, 0]^T$, $\bar{\mathbf{F}}_{\mathbf{n1}} = [0, 1\text{N}, 0]^T$, $\bar{\mathbf{F}}_{\mathbf{n1}} = [0, 0, 1\text{N}]^T$. Up to down: $n = B - 1$, $n = B$, $n = B + 1$

Fig. 2 illustrates the radiation directivities from the row k caused by its interaction with the row l. The same linear scale is used for all directivity patterns. The downstream row has $B^{(k)} = 9$ blades. The upstream row l is assumed to generate radial, tangential or axial forces on the row k. The row k was discretized into a single radial location ($I = 1$) at $R_0 = 5$ cm. The far-field acoustic pressure was calculated using Eq. (10) at J equally spaced points on a spherical surface centered on the fan. To respect the far-field condition, the ratio between the radius of the sphere and the radial location of the sources was $R/R_0 = 100$, $\Omega^{(k)} = 50$ rad.s^{-1}, $\Omega^{(l)} = 1$ rad.s^{-1} and $m = 1$. The radiations were calculated for unitary radial forces $\bar{\mathbf{F}}_{\mathbf{n1}} = [1\text{N}, 0, 0]^T$ (left of Fig. 2), unitary tangential forces $\bar{\mathbf{F}}_{\mathbf{n1}} = [0, 1\text{N}, 0]^T$ (middle of Fig. 2) and unitary axial forces $\bar{\mathbf{F}}_{\mathbf{n1}} = [0, 0, 1\text{N}]^T$ (right of Fig. 2) for $B - 1 \le n \le B + 1$. The radiation from unitary forces having circumferential order $n < B - 1$ and $n > B + 1$ are not presented in Fig. 2, since their radiations are negligible for the parameters chosen in this simulation. Fig. 2 shows that radial and tangential forces exhibits almost the same "donut" directivity patterns for $n = B - 1$ and $n = B + 1$ (the magnitude is null along $\mathbf{e_3}$, i.e. in the axial direction) and their radiation are low or null for $n = B$. The radiated directivity from axial forces is an axial dipole for $n = B$, but the radiation of axial forces are low for $n = B - 1$ and $n = B + 1$. In practice, the axial forces must be dominant for a well-designed axial fan.

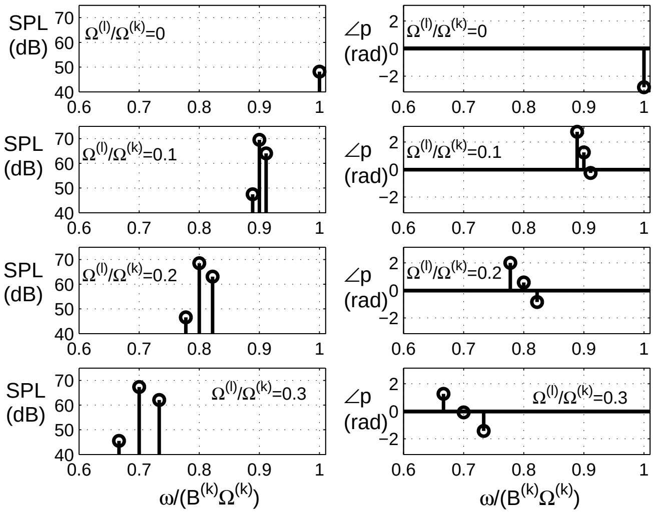

Figure 3: Acoustic pressure $p_{\omega j}^{(k)\leftarrow(l)}$ as a function of the dimensionless frequency $\omega/(B\Omega^{(k)})$ at $\mathbf{x_j} = (R, \pi/4, 0)$ for $\bar{\mathbf{F}}_{\mathbf{n1}} = [0.2\text{N}, 0.3\text{N}, 0.5\text{N}]^T \forall n \in [B-1, B+1]$. Left:SPL, right:phase. Up to down : $\Omega^{(l)}/\Omega^{(k)} = [0, 0.1, 0.2, 0.3]$.

Fig. 3 illustrates the frequency shifts due to the relative rotational speed of rows k and l for various ratio $\Omega^{(l)}/\Omega^{(k)}$, with $\Omega^{(k)} = 50$ rad.s^{-1} and $m = 1$. The far field location point was $(5, \pi/4, 0)$ so that radial, tangential and axial forces radiate. The force vector was $\bar{\mathbf{F}}_{\mathbf{n1}} = [0.2\text{N}, 0.3\text{N}, 0.5\text{N}]^T$. The larger $\Omega^{(l)}/\Omega^{(k)}$, the spreader the modulated frequency content. The left, middle and right frequency peaks shown in Fig. 3 correspond to the circumferential orders $n = B + 1$, $n = B$ and $n = B - 1$ respectively. For $\Omega^{(l)} = 0$, all the circumferential orders of the force interfere at the blade passage frequency $B\Omega^{(k)}$.

3 Experiments

A rectangular obstruction (Fig. 4) is proposed to evaluate the ability of the modulation method proposed in this paper, to reveal the modal content of the forces generated by an interaction between an obstruction and a rotor.

3.1 Set up

In the experiments, the multi-row configuration was (from upstream to downstream, Cf. Fig. 4):

- Row 1: Asymmetric stationary Inlet, $\Omega^{(1)} = 0$
- Row 2: Rotating obstruction, $\Omega^{(2)} \neq 0$
- Row 3: Rotor, $\Omega^{(3)} \neq \Omega^{(2)}$
- Row 4: Stationary radiator, $\Omega^{(4)} = 0$

The stationary inlet flow is considered as a first equivalent-row. The rotor wake that impinges on the radiator and the non-homogeneous flow coming from the inlet (except from

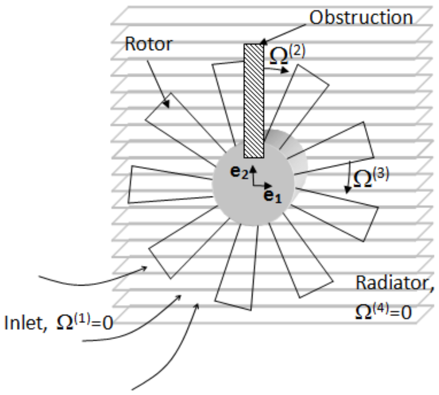

Figure 4: Multi-row configuration

the rotating obstruction) produces sound radiation $\left[\tilde{p}_p(\mathbf{x},\omega)\right]^{(4)\leftarrow(3)}$ and $\left[\tilde{p}_p(\mathbf{x},\omega)\right]^{(3)\leftarrow(1)}$ respectively, at frequencies $mB\Omega^{(3)}$.

The rotating obstruction wakes impinging on the rotor produce sound radiation $[\tilde{p}_s(\mathbf{x},\omega)]^{(3)\leftarrow(2)}$ at frequencies $mB\Omega^{(3)} - n\Omega^{(2)}$.

Assuming linear superposition of the sound radiations, the total sound radiation occurs at the frequencies $mB\Omega^{(3)}$ and $mB\Omega^{(3)} - n\Omega^{(2)}$. Therefore, sound radiation coming from the rotating obstruction can be distinguished in the frequency response of the total sound field provided $\Omega^{(2)} \neq 0$ and $\Omega^{(2)} \neq \Omega^{(3)}$.

A largely subsonic fan rotating at $\Omega^{(3)} = 43 rad.s^{-1}$ was installed in the hemi-anechoic chamber with foam on the ground to prevent the strong effect of the ground reflection on the tonal noise radiation. The rotor had $B^{(3)} = B = 9$ regularly spaced blades and the tip Mach number is $M_t = 0.04$. On the upstream side of the fan, a positioning device allows for the rectangular obstruction to be moved in the azimuthal direction. The obstruction was made of Plexiglas.

The sampling frequency of the sound pressure acquisition system was set to 44100 Hz. A sufficiently long time window T =20s of the measured far field sound pressure was used, in order to obtain a spectral resolution ($\Delta f = 0.25$ Hz for 5 averages) sufficient to separate the frequencies in the spectra. Moreover, order tracking of the time signals were performed to concentrate the energy in the averaged blade passage frequency, in order to avoid the frequency spreading of the BPF tone due to irregularities in the rotational speed of the fan induced by the electrical motor. The azimuthal velocity of the obstruction was $\Omega^{(2)} = 2\pi$ rad.s^{-1} (in the same direction as the rotor), so that the frequencies radiated by the interaction between the rotating obstruction and the rotor are shifted to the left in the acoustic spectrum. This frequency shift was large enough for the two tones to be well separated in the sound pressure frequency response.

3.2 Results

The modulation spectrum around BPF is presented in Fig. 5-a. As expected, the modulation spectrum is single-sided. The radiation at $B\Omega^{(3)}$ is caused by the interaction between the rotor and its fixed environment. This frequency is traditionally called blade passage frequency (BPF). The frequency content caused by the modulation are spread around the central frequency $B\Omega^{(3)} - B\Omega^{(2)}$, that corresponds to the

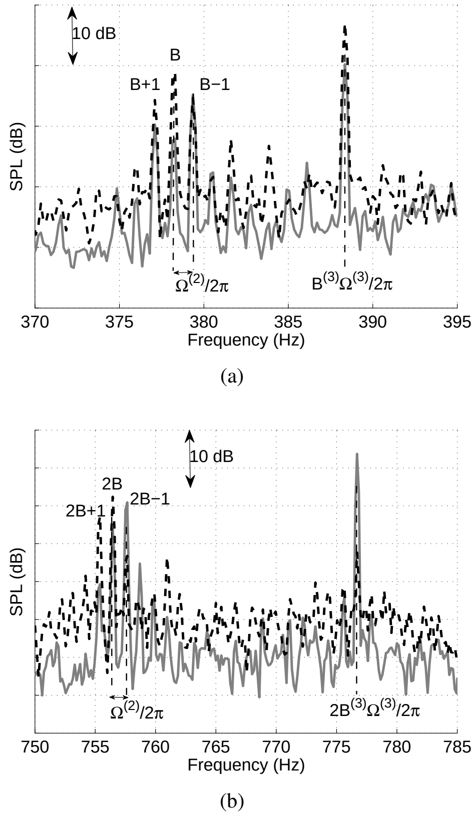

Figure 5: Modulation spectrum, a) around BPF and b) around 2BPF. Black dotted line : microphone in the axial direction and grey plain line : microphone in the radial direction

radiation of the B^{th} mode of the unsteady blade forces. The B-mode radiation is higher in the axial direction than in the radial direction. The intense radiation of this mode in the axial direction can be anticipated from Eq. (8) and from the directivities illustrated in Fig. 2. However, a small effect of the mode B is observed in the radial direction (11 dB less than in the axial direction), which is not predicted by the free field theory. As expected, the radiation of the modes $(B-1)$ and $(B+1)$ contribute to the radiation in the radial direction. The modes $(B-1)$ and $(B+1)$ also contribute to the in-axis radiation, which is not expected by the model proposed in this paper. Similar trends have been observed for a $(B-1)$ sinusoidal obstruction in [8]. These non-expected acoustic contributions may be explained by free field conditions that are not fully respected due to the presence of a large radiator in the downstream flow field of the fan, which can act as a diffracting screen or as an aeroacoustic source (non axial). Several acoustic signatures of modes $n < B-1$ and $n > B+1$ can be seen in the spectrum shown in Fig. 5-a, however, their contribution are small. This can be explained by the Bessel functions in Eq. (8). They act as spatial band pass filters centered on circumferential order mB, for the Bessel function $J_{mB^{(k)}-n}(.)$, and centered on order $(mB-1)$ and $(mB+1)$, for the derivative of the Bessel function $(J'_{mB^{(k)}-n}(.))$. The band pass filters are sharp for small argument of the Bessel functions and are smooth for large argument. This spatial bandpass filtering explain the "bell shape" centered on frequency $B\Omega^{(3)} - B\Omega^{(2)}$ in the acoustic spectra shown in Fig. (5-a).

The modulation spectrum around 2BPF is presented in Fig. 5-b. The radiation at $2B\Omega^{(3)}$ is caused by the interaction between the rotor and its fixed environment. The frequency content caused by the modulation are spread around the central frequency $2B\Omega^{(3)} - 2B\Omega^{(2)}$, that corresponds to the radiation of the mode $2B$ of the unsteady forces. The radiation of the mode $2B$ is higher in the axial direction than in the radial direction, as expected in Eq. (8). However, as in the case of the BPF radiation, a small effect of the mode $2B$ is observed in the radial direction (7 dB less than in the axial direction), which is not predicted by the free field model. As expected, the mode $(2B - 1)$ has a high contribution to the acoustic radiation in the radial direction and a small contribution in the axial direction. Surprisingly, the mode $(2B + 1)$ has a strong contribution to acoustic radiation in the axial direction and a small contribution in the radial direction. The low contribution of the mode $2B + 1$ at the radial acoustic measurement point can comes from destructive interference between the radial and the tangential force radiations; and the non-expected acoustic contributions of the modes (2B-1) and (2B+1) at the axial acoustic measurement point may be explained by free field conditions that are not fully respected, due to the presence of a large radiator in the downstream flow field of the fan. As shown before for the BPF modulation, the spatial band-pass filtering caused by the Bessel functions in Eq. (8) can explain the "bell shape" of the spectrum centered on frequency $2B\Omega^{(3)} - 2B\Omega^{(2)}$ in Fig. (5-b).

The modes $B - 1$, B and $B + 1$ of the unsteady forces generated by the rectangular obstruction/rotor interaction mostly contribute to the noise radiation around BPF and the modes $(2B - 1)$, $2B$ and $(2B + 1)$ mostly contribute to the noise radiation around 2BPF.

One have to keep in mind that as long as the obstruction location is fixed, every mode of the unsteady forces generated by the interaction between the obstruction (or a stator) and the rotor (that radiate sound at different frequencies when the obstruction is rotated) interfere, as illustrated in Fig. 3, to radiate at the BPF and its harmonics.

4 Conclusion

To distinguish the different interactions leading to tonal noise in the acoustic spectrum, an original approach has been presented in this paper, consisting of rotating a quasistatic part (e.g. an obstruction or a stator). An analytical model has been developed to take into account relative rotation motions between a number of rotors, based on the rotating dipole formula. This model shows that the acoustic radiation due to the interaction between a rotating row l and the rotor (row k) shifts in the spectrum at frequencies $mB\Omega^{(k)} - n\Omega^{(l)}$, where $\Omega^{(k)}$ and $\Omega^{(l)}$ are the rotational speed of rows k and l respectively and n is the order of the unsteady forces decomposed in circumferential Fourier series. Using this modulation effect, every circumferential modes n radiate at different frequencies in the acoustic spectrum. The radiation due to the interaction between the rotor and all the other static components remains at frequencies $mB\Omega^{(k)}$. The two analytical models proposed by Lowson [1], conventionally used to calculate rotor noise and stator noise, have been unified so that a stator can be seen as a "non-rotating rotor". Reciprocally, a rotor can be seen as a "rotating stator".

The acoustic modulation effect can be used to estimate the circumferential modal content of the unsteady blade forces, generated by the interaction between a stator and a rotor, that radiates noise. Based on this modal content, the control of the most radiating circumferential orders can be targeted. The modulation effect also provides a method to identify the secondary noise generated by the interaction between a rotor and an upstream control obstruction designed to target one or more modes [8].

The discretization of the modulation equation can lead to better conditioned inverse problems to estimate the aeroacoustic tonal noise sources from measured far field acoustic pressures. Since every circumferential order of the unsteady forces radiates at different frequencies, the formulation proposed in this paper allows low-rank matrices to be inverted, with better conditioning number. Thus, less microphones are needed to measure the radiated sound field.

References

[1] M.V. Lowson, "Theoretical Analysis of Compressor Noise", *Journal of the Acoustical Society of America* **47**(1), 371-385 (1968)

[2] P.M. Morse, K.U. Ingard, *Theoretical acoustics*, Princeton University Press, NJ, USA (1968)

[3] W.K. Blake, *Mechanics of Flow Induced Sound and Vibration, Vol. 2, Complex Flow Structure Interactions*, Academic Press Inc. (1974)

[4] M.E. Goldstein, *Aeroacoustics*, McGraw-Hill International Book Company (1976)

[5] A. Carazo, M. Roger, M. Omais "Analytical prediction of wake-interaction noise in counter-rotation open rotor", *17th AIAA/CEAS Aeroacoustics Conference* Portland, Oregon, USA (2011)

[6] S. Khelladi, S. Kouidri, F. Bakir, R. Rey, "Predicting tonal noise from a high rotational speed centrifugal fan", *Journal of Sound and Vibration* **313**, 113-133 (2008)

[7] A. Gerard, A. Berry, P. Masson, Y. Gervais, "Evaluation of Tonal Aeroacoustic Sources in Subsonic Fans Using Inverse Models", *American Institute of Aeronautics and Astronautics Journal* **45**(1), 98-109 (2006)

[8] A. Gerard, S. Moreau, A. Berry, P. Masson, "Multi modal obstruction to control tonal fan noise: Theory and experiments", *ISROMAC 2012* Honolulu, Hawai, USA (2012)